



Gearbox Reliability Collaborative Gearbox 1 Failure Analysis Report

December 2010 – January 2011

R. Errichello and J. Muller
GEARTECH
Townsend, Montana

NREL is a national laboratory of the U.S. Department of Energy, Office of Energy Efficiency & Renewable Energy, operated by the Alliance for Sustainable Energy, LLC.

Subcontract Report
NREL/SR-5000-53062
February 2012

Contract No. DE-AC36-08GO28308

Gearbox Reliability Collaborative Gearbox 1 Failure Analysis Report

December 2010 – January 2011

R. Errichello and J. Muller
GEARTECH
Townsend, Montana

NREL Technical Monitor: J. Keller
Prepared under Subcontract No. LEE-7-77535-01

NREL is a national laboratory of the U.S. Department of Energy, Office of Energy Efficiency & Renewable Energy, operated by the Alliance for Sustainable Energy, LLC.

NOTICE

This report was prepared as an account of work sponsored by an agency of the United States government. Neither the United States government nor any agency thereof, nor any of their employees, makes any warranty, express or implied, or assumes any legal liability or responsibility for the accuracy, completeness, or usefulness of any information, apparatus, product, or process disclosed, or represents that its use would not infringe privately owned rights. Reference herein to any specific commercial product, process, or service by trade name, trademark, manufacturer, or otherwise does not necessarily constitute or imply its endorsement, recommendation, or favoring by the United States government or any agency thereof. The views and opinions of authors expressed herein do not necessarily state or reflect those of the United States government or any agency thereof.

Available electronically at <http://www.osti.gov/bridge>

Available for a processing fee to U.S. Department of Energy and its contractors, in paper, from:

U.S. Department of Energy
Office of Scientific and Technical Information
P.O. Box 62
Oak Ridge, TN 37831-0062
phone: 865.576.8401
fax: 865.576.5728
email: <mailto:reports@adonis.osti.gov>

Available for sale to the public, in paper, from:

U.S. Department of Commerce
National Technical Information Service
5285 Port Royal Road
Springfield, VA 22161
phone: 800.553.6847
fax: 703.605.6900
email: orders@ntis.fedworld.gov
online ordering: <http://www.ntis.gov/help/ordermethods.aspx>

Cover Photos: (left to right) PIX 16416, PIX 17423, PIX 16560, PIX 17613, PIX 17436, PIX 17721



Printed on paper containing at least 50% wastepaper, including 10% post consumer waste.

DISCLAIMER

This report may contain certain recommendations for increasing load capacity and improving reliability of the subject gear drive. The recommendations are general guidelines that are for the sole purpose of showing what can be achieved. They must not be construed as specific design recommendations. The manufacturer is solely responsible for the design of the gear drive, and GEARTECH accepts no liability for the design.

Background

Unintended gearbox failures have a significant impact on the cost of wind farm operations. In 2007, NREL initiated the Gearbox Reliability Collaborative (GRC). The project combines analysis, field testing, dynamometer testing, condition monitoring, and the development and population of a gearbox failure database in a multi-pronged approach to determine why wind turbine gearboxes do not achieve their expected design life. The collaborative of manufacturers, owners, researchers, and consultants focuses on gearbox testing and modeling and the development of a gearbox failure database. Collaborative members also investigate gearbox condition monitoring techniques. Data gained from the GRC will enable designers, developers, and manufacturers to improve gearbox designs and testing standards and create more robust modeling tools.

GRC project essentials include the development of two identical, heavily instrumented representative gearbox designs. Knowledge gained from the field and dynamometer tests conducted on these gearboxes builds an understanding of how the selected loads and events translate into bearing and gear response. One of the gearboxes was installed in a turbine at the Ponnequin wind farm and put into unattended operation on September 14, 2009. The test was stopped on October 5, 2009 due to bearing temperature exceedances and reports of oil loss from the gearbox. An inspection on October 6, 2009, revealed that the high-speed stage gear teeth showed signs of significant overheating. It was determined that testing should be suspended to avoid the potential for catastrophic gearbox failure. Subsequently, the gearbox was removed from the turbine and shipped back to NREL. After conducting a limited set of condition monitoring tests in the NREL dynamometer, the gearbox was sent to The Gear Works for disassembly and inspection [1]. The results of this disassembly and inspection are reported herein.

Introduction

On December 27-30, 2010 and January 3-7, 2011, Robert Errichello and Jane Muller inspected one Jahnle-Kestermann (JAKE) gearbox at The Gear Works in Seattle, Washington. The root cause of the loss of oil is unknown and, therefore, not addressed in this report. In both instances, a temperature sensor on a high-speed pinion (HSP) bearing signaled a wind turbine shutdown. This report summarizes the results of the inspection of the gearbox and contains photographs of the failed components.

Nomenclature

Table 1 shows nomenclature used in this report.

Table 1- Nomenclature	
ANN	Annulus gear
CAR	Carrier
CRB	Cylindrical roller bearing
fcCRB	Full complement cylindrical roller bearing
HS	High speed
HSG	High-speed gear
HSP	High-speed pinion
INT	Intermediate
INTG	Intermediate gear
INTP	Intermediate pinion
IR	Inner ring
LS	Low speed
OR	Outer ring
SUN	Sun pinion
TRB	Tapered roller bearing

Nameplate data

Table 2 shows nameplate data for the gearbox.

Table 2- Nameplate data	
Jahnel-Kestermann Getriebewerke Bochum G.m.b.H. D44789 Bochum	
Gear type	PSC 1000-48/60 year of man. 1999
Serial No.	31.98.3813.12.07
Power rating	800 kW
Rotational speeds	22.21/1810 rpm
Gear ratio	1:81.491
Oil type	TRIBOL 1510/320
Oil capacity	~ 100 litres oil ISO-VG 320

Application data

Table 3 shows application data.

Table 3- Application data	
TURBINE DATA	
Site/project:	Ponnequin wind farm
Wind turbine model:	NM750/48
Wind turbine pad no:	12
Power rating:	750 kW
Rotor diameter:	48 m
Rotor fixed pitch or variable:	Fixed
Brake type:	HS shaft disk
Brake torque rating:	
HS coupling type:	Centa CL-60-002-60360 complete link set (CCW) Ref: Drawing #19-60360-00-2 Complete set of links – 2x5 per side
LS coupling type:	Shrink disk
SERVICE HISTORY	
Start-up date:	September 14, 2009
Overhaul date:	None
Shutdown date:	September 23, 29, 30 2009 and October 1, 2, 7, 2009
Runtime hours:	
Production kWh:	
No. of brake stops:	42
FAILURE DATA	
How was failure discovered:	Turbine faulted for hot HSP bearing
Any unusual conditions or events:	Gearbox lost oil on September 23 and October 5, 2009
No. of gearboxes failed:	1
No. of gearboxes running:	2
LUBRICANT DATA	
Manufacturer product:	Castrol Optigear Synthetic X 320
Viscosity ISO VG:	320
Gearbox capacity (liters):	144
Date oil last changed:	October 5, 2009
Lab analyses available:	Filter element analysis
Oil cooler installed:	Yes
Online filter installed:	Yes
Offline filter installed:	Yes
Oil temperature in sump:	

Shaft endplay

Table 4 shows the shaft endplay that was measured before disassembling the gearbox.

Table 4- Shaft endplay	
Shaft	Endplay (mm)
HS	0.15
INT	0.13
LS	0.41
SUN	1.32
CAR	0.51

Lubricant

The lubricant was Castrol Optigear Synthetic X 320.

Description of gear arrangement

Figures 1-2 show the gear and bearing arrangement. Table 5 details the bearing data.



Figure 1- Exploded view of the gearbox

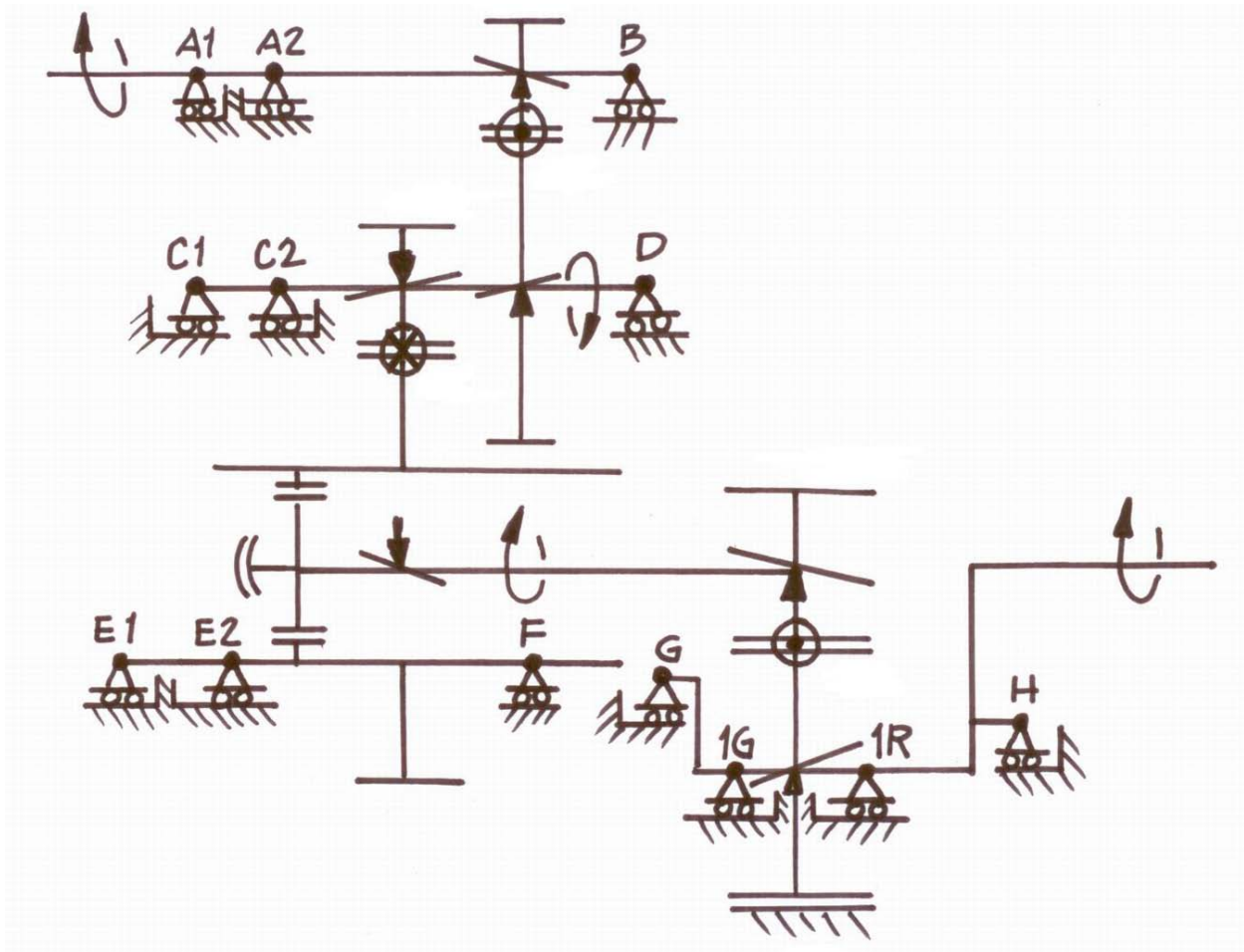


Figure 2- Gear and bearing arrangement (not to scale)

Table 5- Bearing data			
Bearing	Type	Manufacturer	Catalog No.
A1	TRB	SKF	32222 J2
A2	TRB	SKF	32222 J2
B	CRB	FAG	NU2220E.M1.C3
C1	TRB	SKF	32032X
C2	TRB	SKF	32032X
D	CRB	FAG	NU2220E.M1.C3
E1	TRB	SKF	32948*
E2	TRB	SKF	32948*
F	fcCRB	INA	SL 18 1856E
G	fcCRB	INA	SL 18 1880 72/K10
H	fcCRB	INA	SL 18 1892E
1G	CRB	FAG	NJ2232E.M1.C3
1R	CRB	FAG	NJ2232E.M1.C3

* These catalog numbers could not be confirmed and were taken from the assembly drawing's bill of material.

Findings

1. The primary failure mode of the HS gearset was severe scuffing. The root cause of the failure was probably lubricant starvation. The wear pattern indicates the HS gear mesh was misaligned causing a higher load at the rotor end of the teeth.
2. The primary failure mode of the sun spline was severe fretting corrosion. The root causes of the failure were probably lubricant starvation and poor load distribution (only about 50% of the teeth carried the load).
3. The primary failure mode of the "O"-ring/hollow shaft seal was severe scuffing and vaporization of the "O"-ring. The root cause of failure was excessive endplay in the TRB bearings E1/E2, which was caused by wear on the bearing locknut due to spinning of the IR of bearing E1.
4. Bearing A1 overheated. Straw-yellow temper color indicates that the temperature reached about 400°F. The root cause of the overheating was probably lubricant starvation.
5. Although the HS gearset, sun spline, and bearing A1 showed evidence of overheating due to lubricant starvation, there was no other evidence that the gearbox ran out of oil. Therefore, the gearbox may have leaked oil, but it did not run completely dry.
6. The IR of bearing D had assembly damage at the roller spacing caused by a cocking of the rollers during blind assembly.
7. The spacer for bearing C1/C2 ORs had assembly damage at the roller spacing caused by interference with the bearing rollers during assembly.
8. The IR of bearing D had corrosion at the roller spacing.
9. The sun spherical thrust rings had small patches of fretting corrosion. The root cause of the fretting corrosion was probably lubricant starvation due to malfunction of the bronze transfer ring.
10. The interface between bearing H OR and the shoulder on bearing cap H had severe fretting corrosion. The root cause of the fretting corrosion was probably the loose fit of bearing H OR.
11. Most gears had some teeth corrosion, with mild to severe fretting. The root cause of the fretting corrosion was parking of the wind turbine.
12. All teeth of the intermediate gearset had a spot of fretting corrosion and scuffing. The root cause of the fretting corrosion and scuffing was probably trapping of debris between a pair of teeth. The hunting gear ratio caused the damage to imprint on all of the teeth in the intermediate gearset.

13. The annulus gear had a 25 mm patch of scuffing. The root cause of the scuffing was probably trapping of debris. The non-hunting gear ratio, with a common factor of three, caused the damage to imprint on every third tooth.
14. The annulus gear wear pattern indicated that the load distribution was heavier at the rotor end of the teeth.
15. The orientation of the annulus gear showed that it was assembled such that the load flanks had prior macropits that were hand dressed.
16. The oil transfer ring for the planet carrier was found cocked and jammed in the carrier. The wear pattern on its rubbing face showed it had only limited contact with the housing over a 50 mm sector. Hand pressure on the transfer ring showed that it was prone to jamming.
17. The oil transfer ring for the hollow shaft did not appear to be jammed. The wear pattern on its rubbing face showed it had nearly 360° contact with the housing. However, hand pressure on the transfer ring showed that it was prone to jamming.
18. It was not possible to obtain accurate torques for the annulus bolts because they had been assembled with Loctite.
19. Upon disassembly, one annulus bolt on the HS housing interface jammed and stripped threads in the annulus gear.
20. The flat washers for the annulus bolts had their outside diameters reduced by machining. This defeated the purpose of the washers and increased contact pressure on the cast iron housings.
21. There was no external V-ring and no felt seal on the HS labyrinth. This allowed the gearbox to breathe through the labyrinth and ingest moisture and dust.
22. There was no external V-ring on the LS labyrinth. This allowed moisture and dust to enter the gearbox.
23. Rust was found on the carrier bore for the rotor shaft and on the OD fit for the shrink ring. These occurred because no rust preventative was applied when the gearbox was removed from the rotor shaft.
24. There was no shield on the inboard side of the pitch tube bearing. This allowed grease to leak out of the bearing into the gearbox.
25. There were no tapped holes or other provisions for handling the hollow shaft. This made assembly and disassembly difficult and increased the risk of assembly damage.
26. There was no space for a puller or other provisions for removing bearing E2 IR from the hollow shaft.

27. There were no provisions for removing bearing E1 and E2 OR from the sleeve.
28. There were no provisions for measuring endplay on the intermediate and hollow shafts.
29. The gasket material used on inspection covers and bearing caps was brittle. This creates a risk that broken fragments of the gasket can enter the gearbox.
30. Dykem spray was used. The coating thickness was too thick and there was excessive overspray on the gear housing and other components.
31. The angular displacement of the axis of the planet carrier relative to the axis of the ANN gear was measured at 0.00073 radians.

Recommendations for Improving the Gearbox Design

1. Add a lubricant spray jet at the outgoing side of the HS gear mesh. Modify the lubrication system such that it monitors system oil pressure and shuts down the wind turbine if the pressure drops below a safe minimum. Inspect the HSP, HSG, and gear housing bores to determine the source of the misalignment of the HS gear mesh.
2. Modify the lubrication system to increase the oil flow rate through the sun spline. Increase the accuracy of the spline teeth to improve tooth-to-tooth load distribution.
3. Use an interference fit on the IR of bearing E1 to prevent spinning of the IR. Revise the design of the locknut such that it applies a high axial clamping force.
4. Review the oil flow rate to bearing A1 and increase the flow rate or oil distribution as necessary to adequately cool the bearing.
5. Review the design of the lubrication system and revise as necessary to prevent lubrication starvation.
6. Review the assembly procedure for bearing D and revise as necessary to avoid assembly damage.
7. Revise the design of the spacer for bearings C1/C2 ORs to avoid assembly damage.
8. Review the design of the lubrication system and revise as necessary to prevent ingress of moisture.
9. Review the design of the lubrication system to ensure adequate oil flow rate to the sun spherical thrust rings.
10. Review the design of the fit of the OR of bearing H and the bearing cap for bearing H and revise as necessary to eliminate fretting corrosion at the interface between bearing H OR and the shoulder on bearing cap H.
11. Review the wind turbine parking procedure and revise as necessary to prevent fretting corrosion.
12. Eliminate debris contamination such as wear debris or gasket material to avoid damage to gear teeth and bearings.
13. Eliminate debris contamination such as wear debris or gasket material to avoid damage to gear teeth and bearings.

14. Review the lead modification for the planet and annulus and revise as necessary to improve load distribution on the planet/annulus gear mesh.
15. Replace the annulus gear with a new gear.
16. Revise the design of the oil transfer ring for the carrier so that it is not prone to jamming. Design a test to measure oil flow rate to the planet bearings.
17. Revise the design of the oil transfer ring for the hollow shaft so that it is not prone to jamming. Design a test to measure oil flow rate to the sun spline.
18. Do not use Loctite on the annulus bolts.
19. Review the access for the annulus bolt that stripped and design tools for assembly/disassembly of the bolt to prevent stripping of bolt threads.
20. Use large diameter hardened steel washers on the annulus bolts. Machine spot faces on the torque arm and HS housing to provide smooth, flat surfaces for the washers.
21. Add an external V-ring and felt seal to the HS labyrinth.
22. Add an external V-ring to the LS labyrinth.
23. Coat the bore and outside diameter of the carrier extension with rust preventative whenever the gearbox is disassembled from the rotor shaft.
24. Use a pitch tube bearing with double shields.
25. Add provisions for handling the hollow shaft.
26. Revise the design of the hollow shaft such that bearing E2 IR is removable.
27. Revise the design of the sleeve and spacer for bearings E1 and E2 to allow removal of the ORs.
28. Add provisions for measuring endplay on the intermediate and hollow shafts.
29. Do not use the current gasket material. Use a rubber gasket on both inspection covers so that the housing surfaces are clean and no sealer is necessary. Use silicone sealer or a ductile gasket material on bearing caps.
30. Do not use Dykem spray. Follow GEARTECH QP8702 for applying Dykem.



Figure No: 3 (NREL PIX 19860)

Scale: 1.5X

Component: HSP

Failure mode: scuffing

Failure mode severity: severe

Description: Flanks have scuffing that is biased toward the rotor end of the pinion and varies from 65 to 105 mm wide in a sinusoidal pattern.



Figure No: 4 (NREL PIX 19861)

Scale: 1.6X

Component: HSP

Failure mode: scuffing

Failure mode severity: severe

Description: Same as Figure 1 except closeup view.

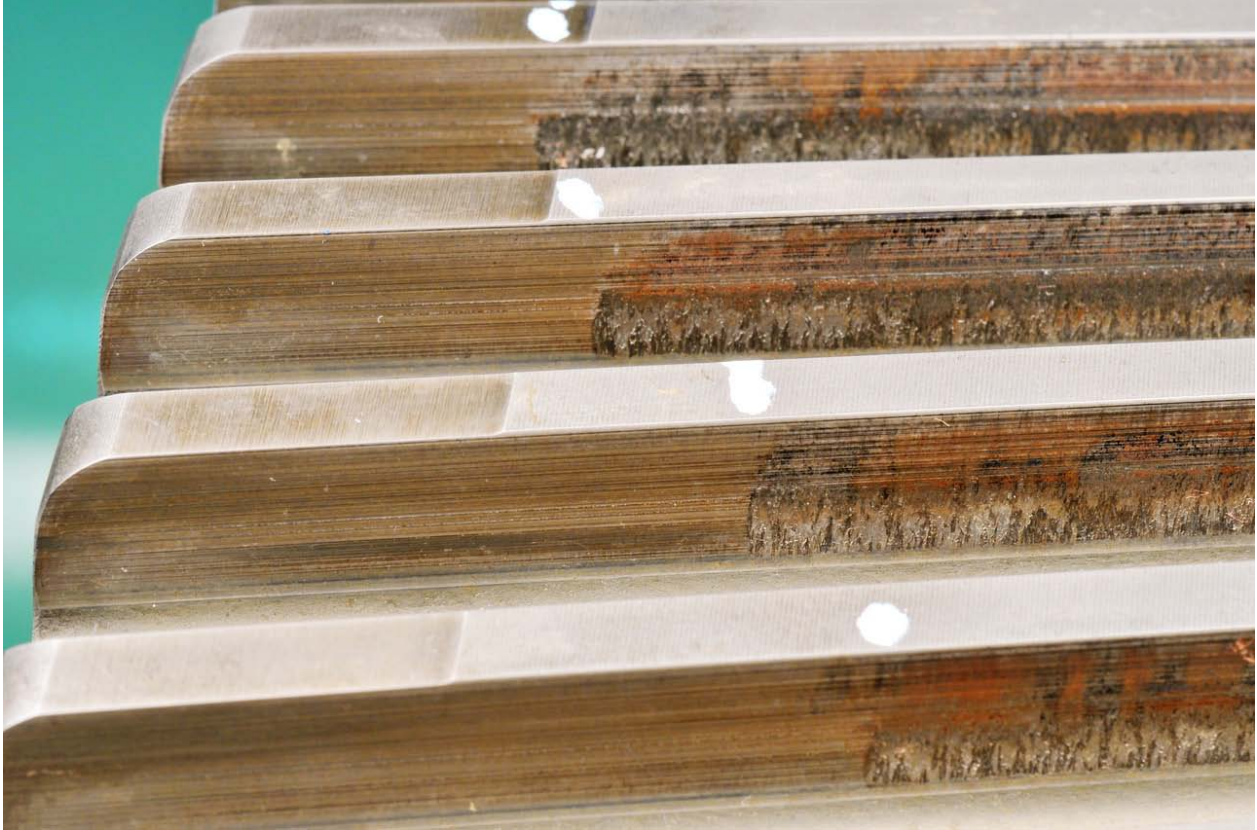


Figure No: 5 (NREL PIX 19871)

Scale: 2.0X

Component: HSG generator end

Failure mode: scuffing

Failure mode severity: severe

Description: Flanks have scuffing that is biased toward the rotor end of the gear and varies from 65 to 105 mm wide in a sinusoidal pattern.



Figure No: 6 (NREL PIX 19872)

Scale: 4.5X

Component: HSG rotor end

Failure mode: scuffing

Failure mode severity: severe

Description: Scuffing is concentrated in the dedenda and corresponds to the scuffing on the pinion addenda. Original grind marks are present in the addenda.



Figure No: 7 (NREL PIX 19852)

Scale: 1.1X

Component: sun spline

Failure mode: fretting corrosion

Failure mode severity: severe

Description: Fretting corrosion is concentrated in the midface and is most severe at the high point of the lead crown. Tooth-to-tooth contact varies from no contact to heavy contact. Only about 50% of the teeth carried the load.

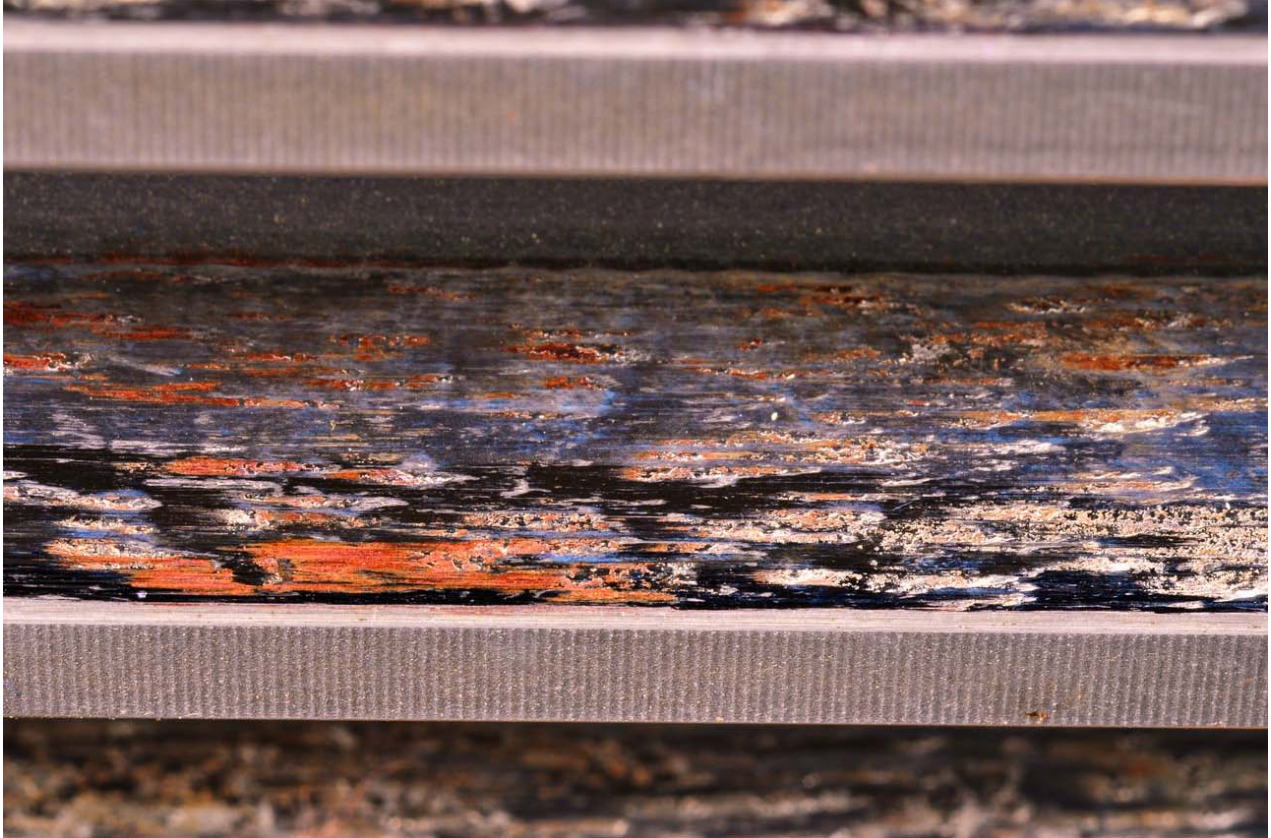


Figure No: 8 (NREL PIX 19853)

Scale: 6.0X

Component: sun spline

Failure mode: fretting corrosion

Failure mode severity: severe

Description: Closeup view of a tooth with severe fretting corrosion. Adhesion between the external sun spline and the hollow shaft internal spline transferred lumps of material from the hollow shaft. Axial sliding broke the welds and deformed the material in the axial direction. The red debris is hematite (Fe₂O₃). Hematite is a polishing agent that created polishing wear that surrounds the fretting damage.

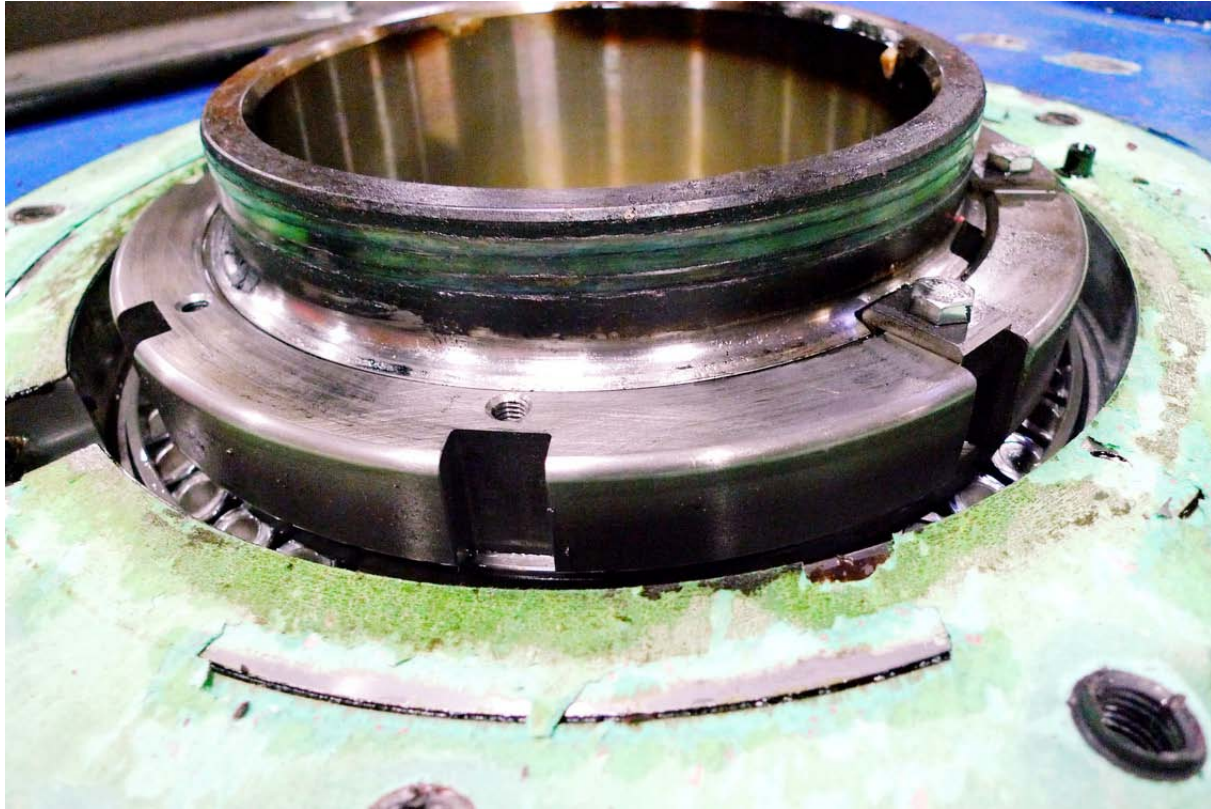


Figure No: 9 (NREL PIX 19837)

Scale: 0.45X

Component: hollow shaft

Failure mode: scuffing

Failure mode severity: severe

Description: View of the hollow shaft extension that rubbed on the “O”-ring seal plate. The rubbing caused severe scuffing on the hollow shaft and “O”-ring seal plate. The “O”-ring vaporized. The green gasket is broken in many places indicating that it is brittle.

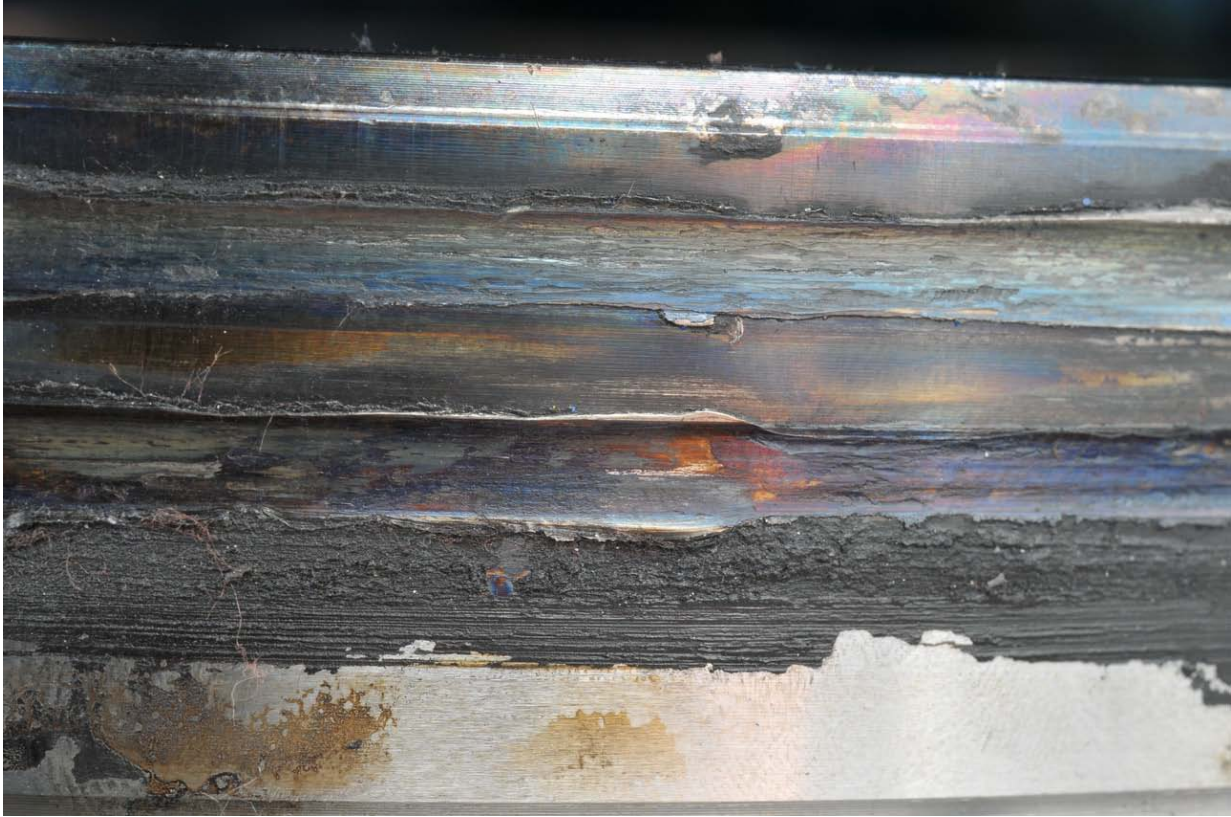


Figure No: 10 (NREL PIX 19875)

Scale: 2.8X

Component: hollow shaft

Failure mode: scuffing

Failure mode severity: severe

Description: Closeup view of the hollow shaft extension that rubbed on the “O”-ring seal plate. The scuffing wore two deep grooves into the hollow shaft. The black coating near the bottom of the photo is debris from the vaporized “O”-ring.



Figure No: 11 (NREL PIX 19838)

Scale: 0.45X

Component: "O"-ring seal plate

Failure mode: scuffing

Failure mode severity: severe

Description: View of the "O"-ring seal plate that rubbed on the hollow shaft. The rubbing caused severe scuffing on the hollow shaft and the "O"-ring seal plate. The "O"-ring vaporized. A lump of melted rubber adhered to the plate. The temper colors near the bore of the "O"-ring seal plate show that the temperature reached at least 700°F.



Figure No: 12 (NREL PIX 19874)

Scale: 2.5X

Component: bearing locknut for bearings E1/E2

Failure mode: abrasion

Failure mode severity: severe

Description: View of the face of the bearing locknut showing severe abrasive wear. Spinning of the IR of bearing E1 caused the bearing E1 IR to rub on the locknut.



Figure No: 13 (NREL PIX 19873)

Scale: 9.6X

Component: bearing locknut for bearings E1/E2

Failure mode: abrasion

Failure mode severity: severe

Description: Closeup view of the face of the bearing locknut. Abrasion removed 0.27 mm from the face of the locknut. The end face of bearing E1 IR also was worn, but to a lesser degree than the locknut.



Figure No: 14 (NREL PIX 19858)

Scale: 2.7X

Component: bearing A1 IR

Failure mode: overheating

Failure mode severity: mild

Description: Mild overheating created straw-yellow temper colors near each end of the IR raceway. The temper colors show that the temperature reached about 400°F.



Figure No: 15 (NREL PIX 19859)

Scale: 1.4X

Component: bearing A1 rollers

Failure mode: overheating

Failure mode severity: mild

Description: Mild overheating created straw-yellow temper colors near each end of the rollers. The temper colors show that the temperature reached about 400°F.

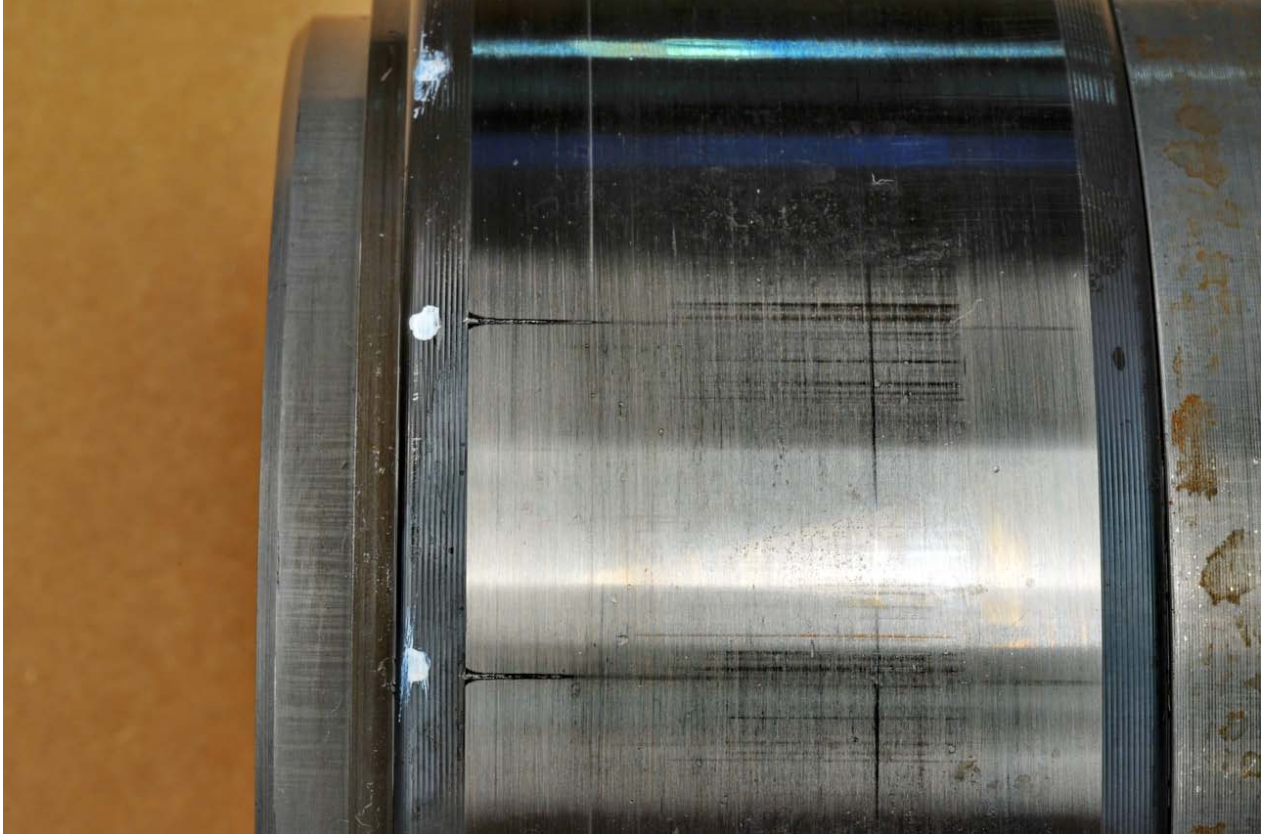


Figure No: 16 (NREL PIX 19864)

Scale: 2.1X

Component: bearing D IR

Failure mode: assembly damage

Failure mode severity: moderate

Description: Three lines of plastic deformation and scuffing at the roller spacing indicate that the rollers cocked and jammed on the IR during assembly.

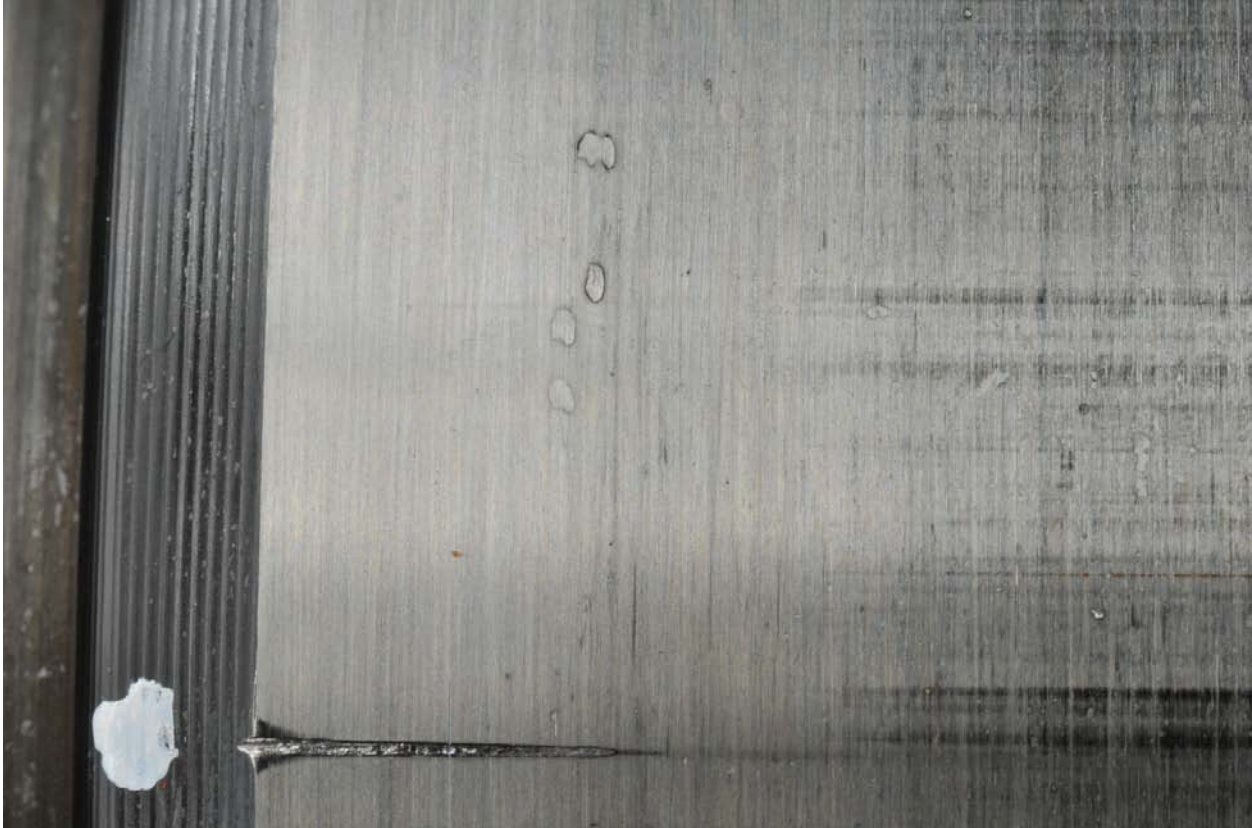


Figure No: 17 (NREL PIX 19865)

Scale: 5.8X

Component: bearing D IR

Failure mode: assembly damage

Failure mode severity: moderate

Description: Closeup view of assembly damage. Debris dents and lines of false brinelling also are shown.



Figure No: 18 (NREL PIX 19866)

Scale: 3.2X

Component: bearing D IR

Failure mode: contact corrosion

Failure mode severity: mild

Description: Closeup view of contact corrosion at the roller spacing. Debris dents, false brinelling, and a circumferential line of abrasion also are shown.



Figure No: 19 (NREL PIX 19867)

Scale: 1.3X

Component: bearing C1/C2 OR spacer

Failure mode: assembly damage

Failure mode severity: severe

Description: Three lines of plastic deformation at roller spacing indicate that the rollers of bearing C1 interfered with the spacer during assembly.

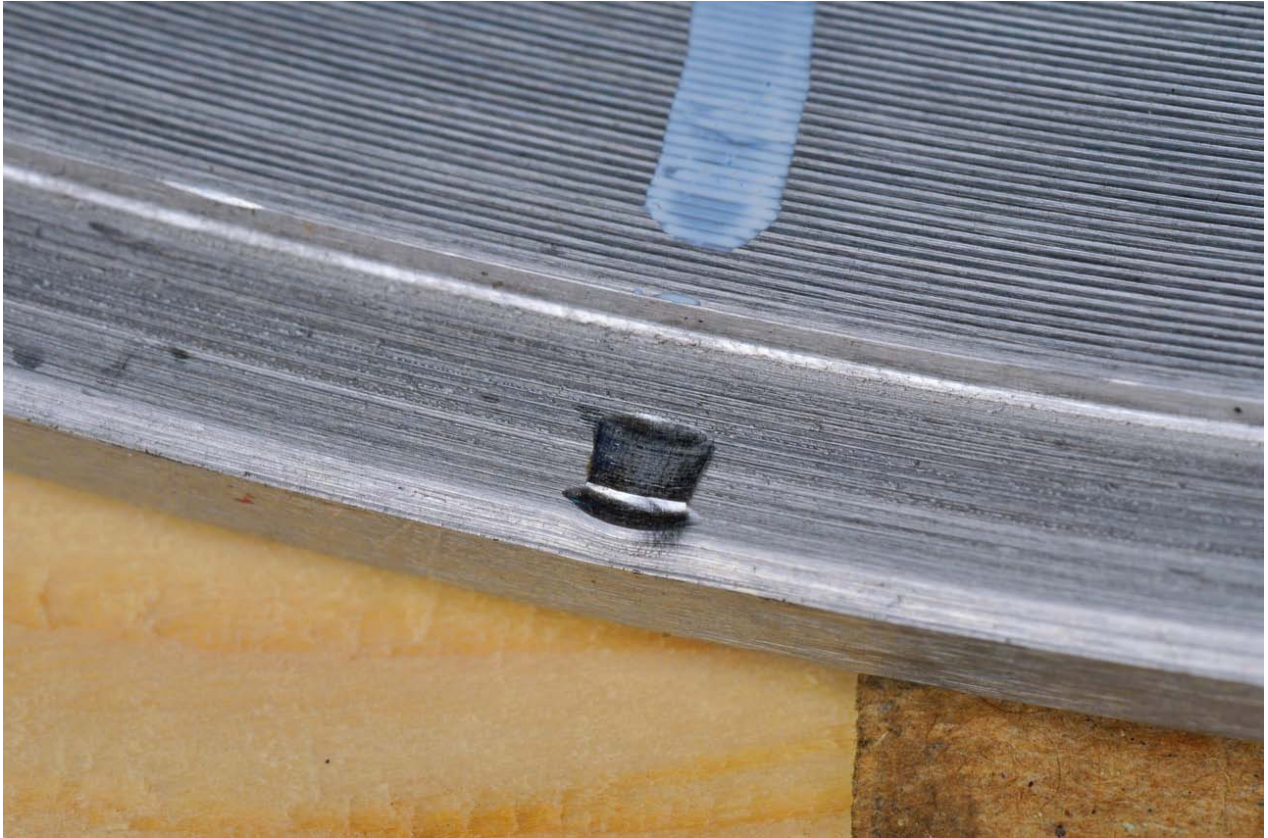


Figure No: 20 (NREL PIX 19868)

Scale: 4.9X

Component: bearing C1/C2 OR spacer

Failure mode: assembly damage

Failure mode severity: severe

Description: Closeup of the dent in the bearing C1/C2 spacer. The dent caused a raised area on the end face of the spacer.



Figure No: 21 (NREL PIX 19846)

Scale: 1.0X

Component: sun upper spherical thrust ring

Failure mode: fretting corrosion

Failure mode severity: moderate

Description: Fretting corrosion occurred in a 60° sector near the outside diameter. The balance of the thrust surface had only mild wear.



Figure No: 22 (NREL PIX 19847)

Scale: 2.5X

Component: sun upper spherical thrust ring

Failure mode: fretting corrosion

Failure mode severity: moderate

Description: Closeup of fretting corrosion.



Figure No: 23 (NREL PIX 19848)

Scale: 1.7X

Component: sun lower spherical thrust ring

Failure mode: fretting corrosion

Failure mode severity: moderate

Description: Fretting corrosion occurred in a 60° sector near the outside diameter. The balance of the thrust surface had only mild wear.



Figure No: 24 (NREL PIX 19849)

Scale: 3.0X

Component: sun lower spherical thrust ring

Failure mode: fretting corrosion

Failure mode severity: moderate

Description: Closeup of fretting corrosion.



Figure No: 25 (NREL PIX 19839)

Scale: 3.0X

Component: bearing H retainer

Failure mode: fretting corrosion

Failure mode severity: severe

Description: Closeup of fretting corrosion. Fretting corrosion occurred in a small sector on the face of the bearing H retainer thrust shoulder that locates bearing H OR.



Figure No: 26 (NREL PIX 19843)

Scale: 1.9X

Component: bearing H OR

Failure mode: fretting corrosion

Failure mode severity: severe

Description: Closeup of fretting corrosion. Fretting corrosion occurred in a small sector on the end face of bearing H OR.

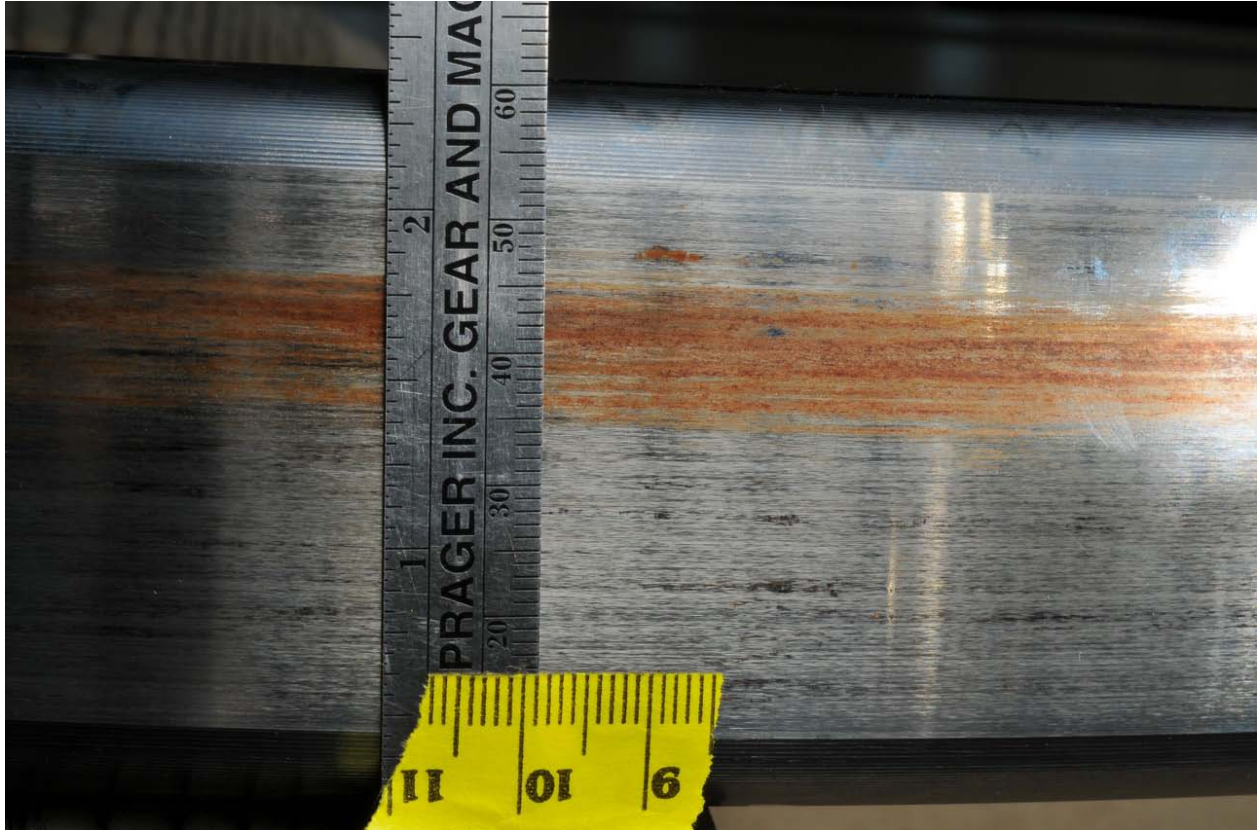


Figure No: 27 (NREL PIX 19844)

Scale: 1.7X

Component: bearing H OR

Failure mode: fretting corrosion

Failure mode severity: severe

Description: Fretting corrosion occurred in a 140° sector on the outside diameter of bearing H OR.



Figure No: 28 (NREL PIX 19850)

Scale: 1.0X

Component: sun pinion

Failure mode: fretting corrosion

Failure mode severity: severe

Description: Fretting corrosion occurred along a line of contact.



Figure No: 29 (NREL PIX 19851)
Scale: 3.2X
Component: sun pinion
Failure mode: fretting corrosion
Failure mode severity: severe
Description: Closeup view of fretting corrosion.

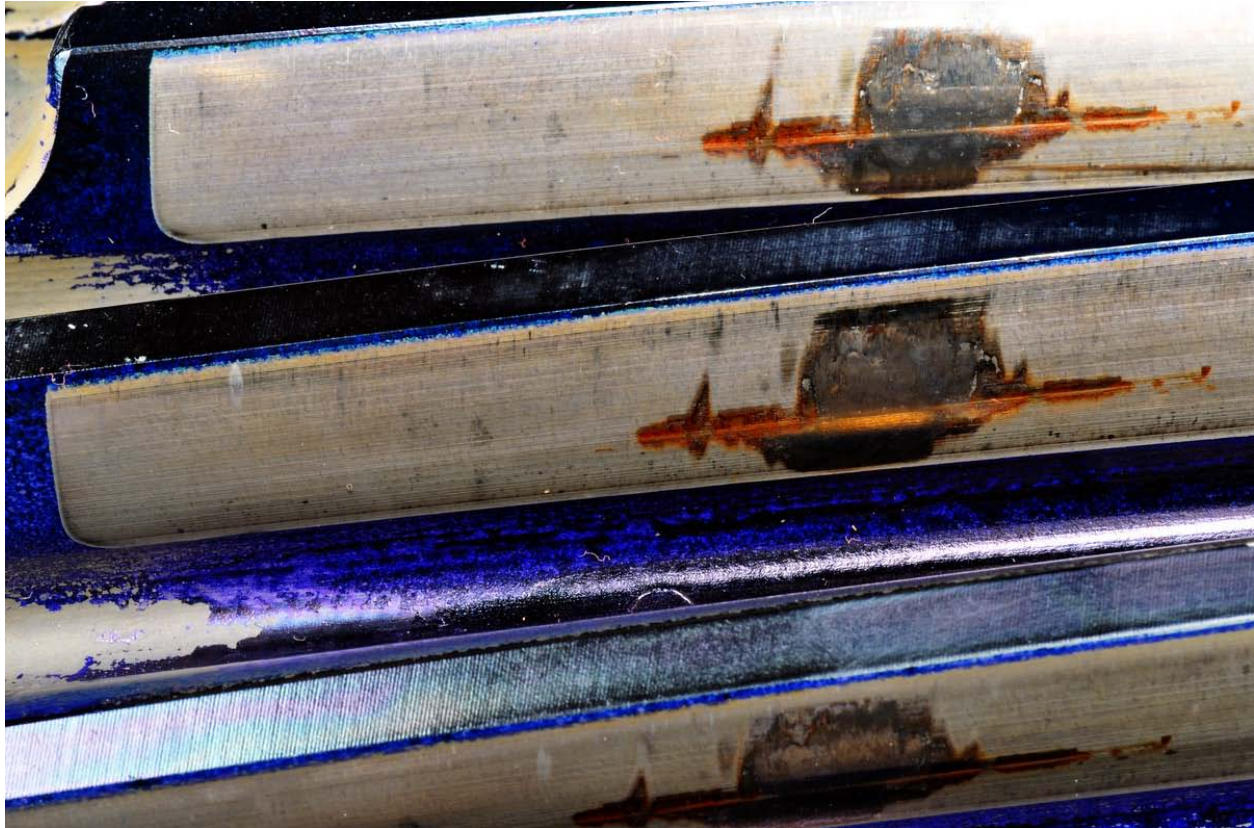


Figure No: 30 (NREL PIX 19862)

Scale: 2.1X

Component: INTP

Failure mode 1: fretting corrosion

Failure mode severity 1: severe

Failure mode 2: polishing wear

Failure mode severity 2: severe (local)

Failure mode 3: scuffing

Failure mode severity 3: severe (local)

Description: Fretting corrosion, polishing, and scuffing. Damage was imprinted on all teeth because the gearset had a hunting gear ratio.

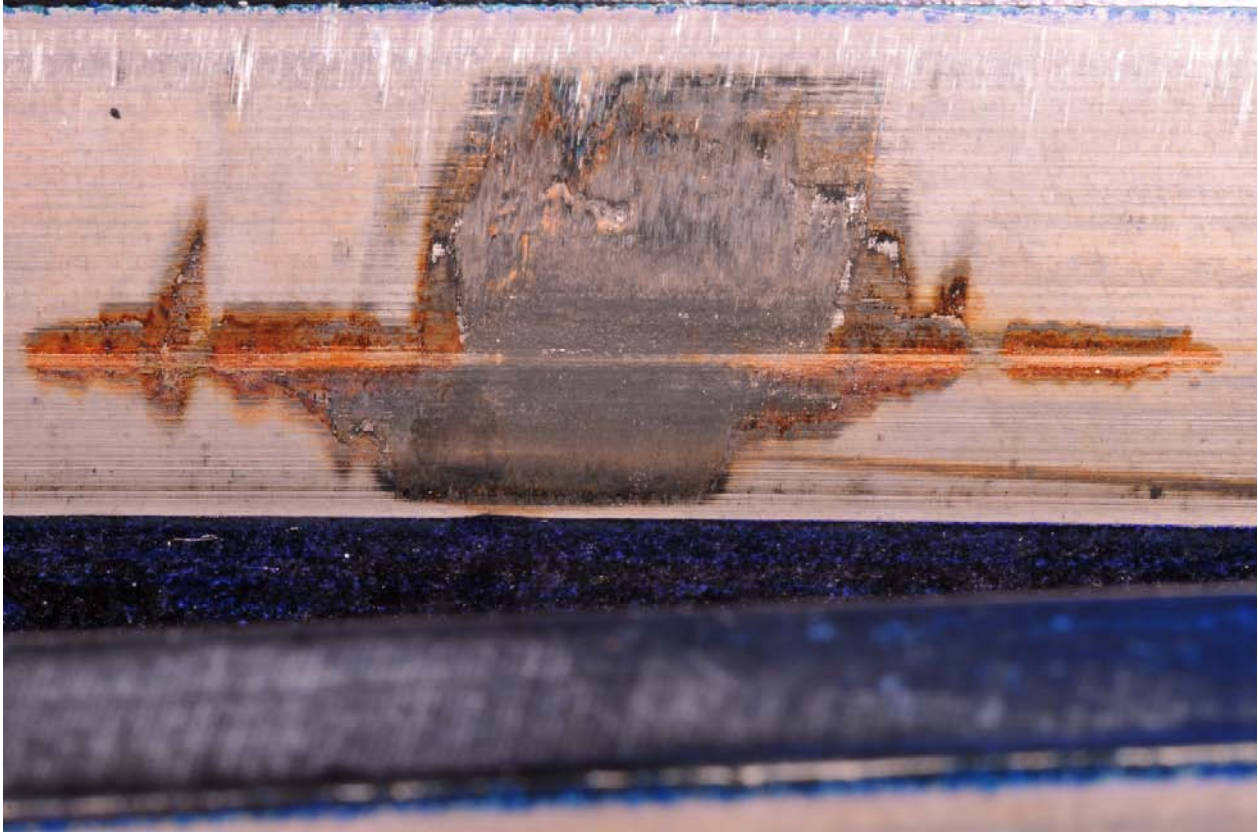


Figure No: 31 (NREL PIX 19863)

Scale: 4.5X

Component: INTP

Failure mode 1: fretting corrosion

Failure mode severity 1: severe

Failure mode 2: polishing wear

Failure mode severity 2: severe (local)

Failure mode 3: scuffing

Failure mode severity 3: severe (local)

Description: Closeup view of the fretting corrosion, polishing, and scuffing.

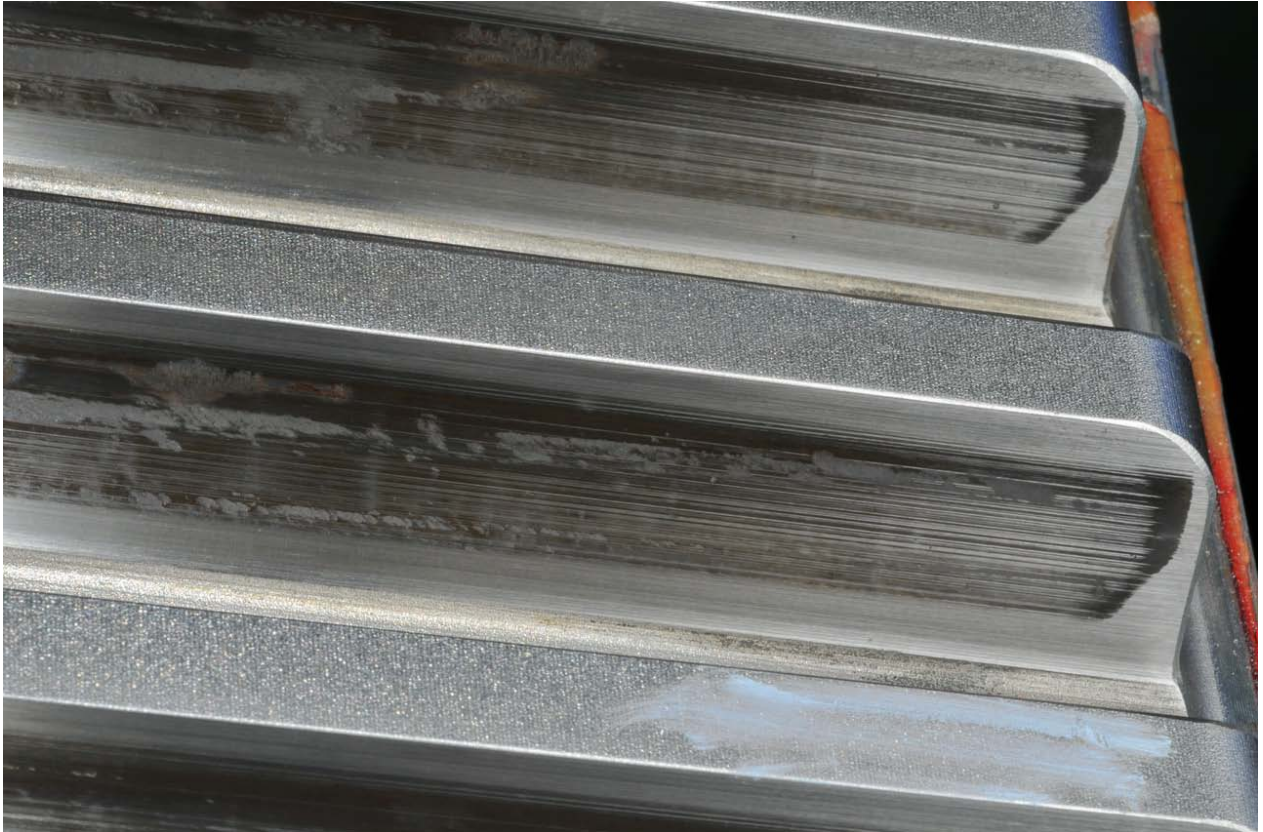


Figure No: 32 (NREL PIX 19854)

Scale: 1.4X

Component: ANN

Failure mode 1: scuffing

Failure mode severity 1: moderate (local)

Failure mode 2: polishing

Failure mode severity 2: moderate

Description: Closeup view of polishing at the generator end of the teeth.



Figure No: 33 (NREL PIX 19855)

Scale: 1.4X

Component: ANN

Failure mode 1: scuffing

Failure mode severity 1: moderate (local)

Failure mode 2: polishing

Failure mode severity 2: moderate

Description: Closeup view of scuffing near the midface of the teeth.

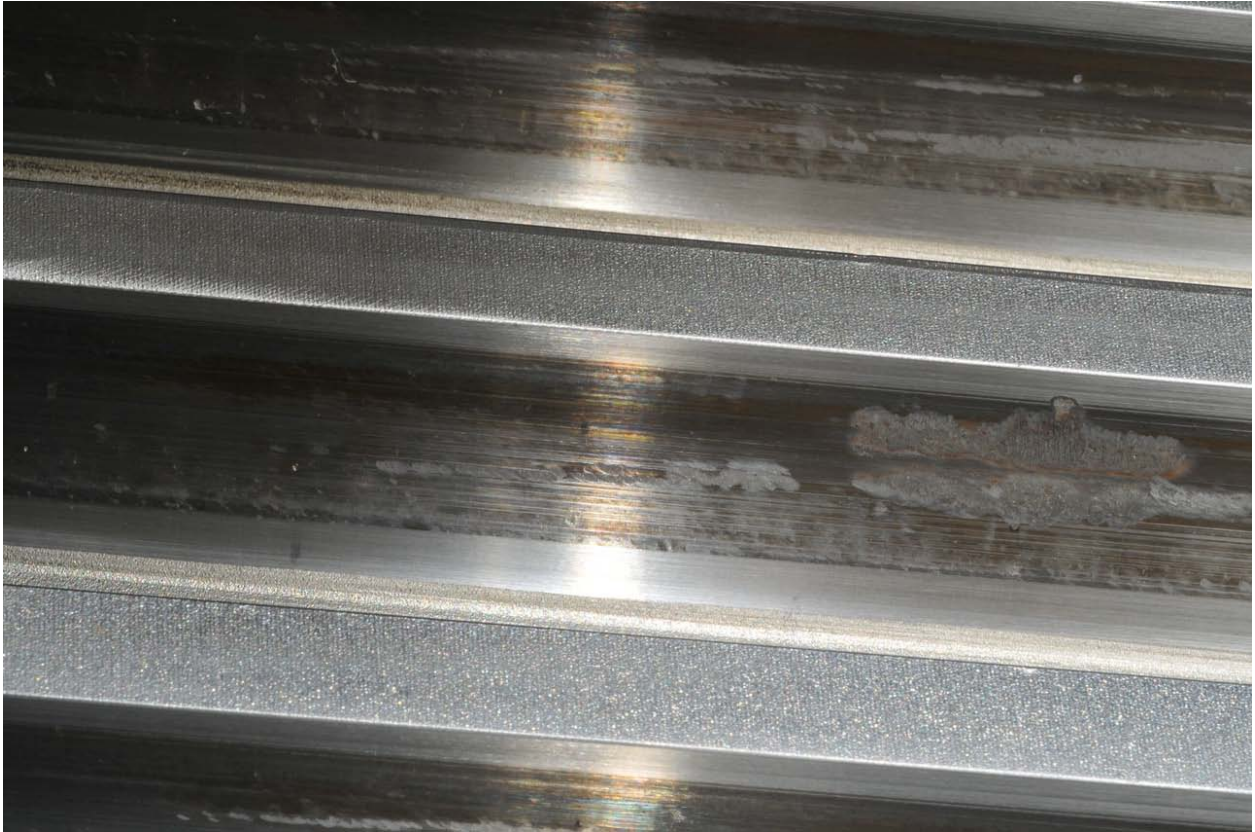


Figure No: 34 (NREL PIX 19856)

Scale: 1.4X

Component: ANN

Failure mode 1: scuffing

Failure mode severity 1: moderate (local)

Failure mode 2: polishing

Failure mode severity 2: moderate

Description: Closeup view of scuffing near the midface of the teeth.



Figure No: 35 (NREL PIX 19857)

Scale: 1.5X

Component: ANN

Failure mode 1: scuffing

Failure mode severity 1: moderate (local)

Failure mode 2: polishing

Failure mode severity 2: severe

Description: Closeup view of severe polishing wear at the rotor end of the teeth. Two original, hand dressed macropits are shown. Polishing wear removed all traces of the grind marks and created a wear step at the end of the contact.



Figure No: 36 (NREL PIX 19840)

Scale: 2.7X

Component: oil transfer ring for carrier

Failure mode: polishing

Failure mode severity: mild (local)

Description: Closeup view of polishing near the outside diameter of the rubbing face. The contact area was only about 50 mm long.



Figure No: 37 (NREL PIX 19841)

Scale: 1.9X

Component: oil transfer ring for carrier

Failure mode: polishing

Failure mode severity: mild (local)

Description: Closeup view of polishing on the outside diameter. The marks occurred when the ring cocked and jammed.



Figure No: 38 (NREL PIX 19842)

Scale: 1.4X

Component: oil transfer ring for carrier

Failure mode: polishing

Failure mode severity: mild (local)

Description: Closeup view of polishing on the bore. The marks occurred when the ring cocked and jammed.



Figure No: 39 (NREL PIX 19845)

Scale: 2,0X

Component: ANN bolt hole

Failure mode: plastic deformation

Failure mode severity: severe

Description: Closeup view of stripped thread. The failure occurred when the bolt jammed during removal.



Figure No: 40 (NREL PIX 19836)

Scale: 1.2X

Component: ANN bolt washer

Failure mode: none

Failure mode severity: none

Description: Closeup view of the bolt and washer. The washer outside diameter had been reduced by machining to a diameter about equal to the bolt shoulder.

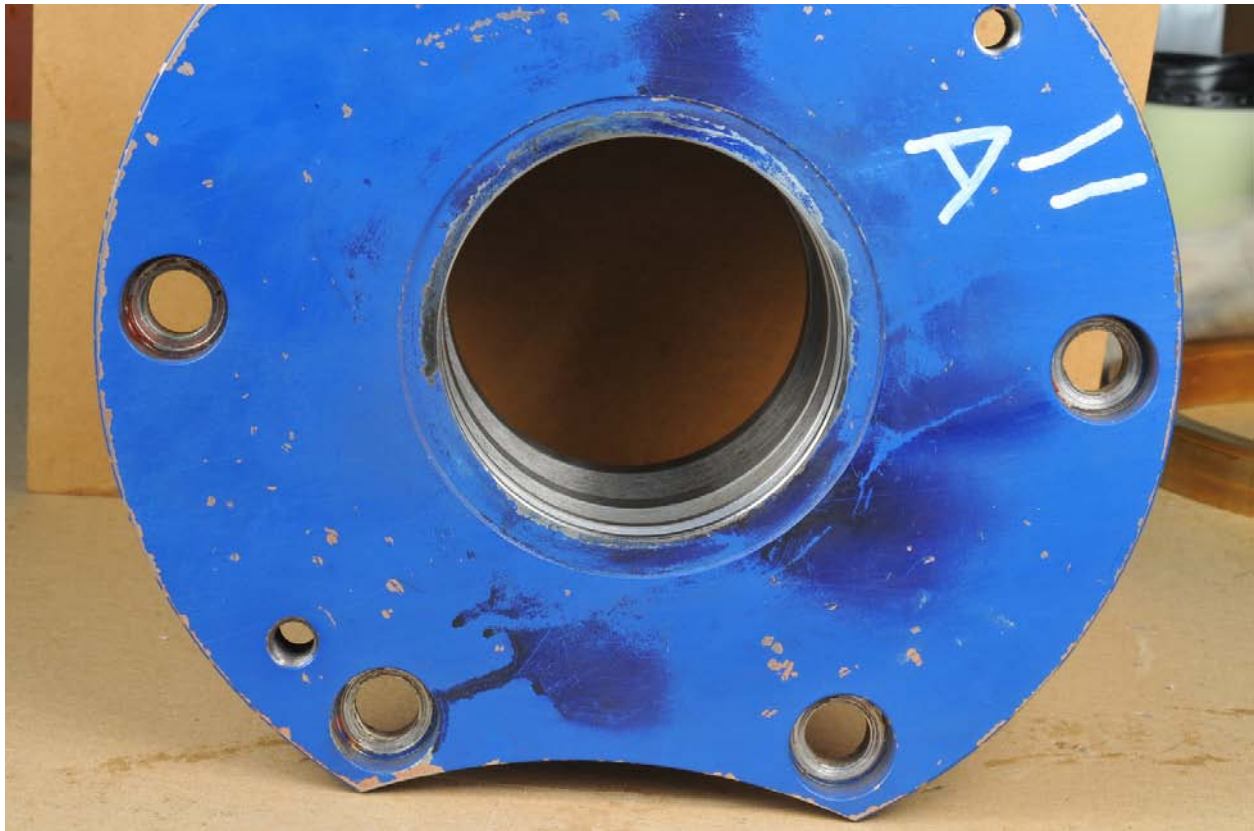


Figure No: 41 (NREL PIX 19869)

Scale: 0.50X

Component: bearing cap A

Failure mode: none

Failure mode severity: none

Description: Closeup view of cap face. There was no V-ring and no wear track from a V-ring.



Figure No: 42 (NREL PIX 19870)

Scale: 1.3X

Component: bearing cap A

Failure mode: none

Failure mode severity: none

Description: Closeup view of felt seal groove. There was no felt seal and no wear track on the HSP from a felt seal.



Figure No: 43 (NREL PIX 19835)

Scale: 0.49X

Component: bearing cap H

Failure mode: none

Failure mode severity: none

Description: Closeup view of cap face. There was no V-ring and no wear track from a V-ring. Oil on the cap face shows minor oil leaks. Rust is evident on the outside diameter of the carrier extension.



Figure No: 44 (NREL PIX 19834)

Scale: 0.30X

Component: complete gearbox

Failure mode: none

Failure mode severity: none

Description: View of experimental setup for measuring displacement of the planet carrier relative to the gear housing. Two dial indicators were mounted on the gear housing, with their probes located on the outside diameter of the carrier extension, to record the movement of the planet carrier.

Discussion

HS gearset scuffing

Figures 3-6 show severe scuffing on the HS gearset. The scuffing is biased toward the rotor end of the pinion, indicating that the HS gear mesh was misaligned. Furthermore, the scuffing varied in a sinusoidal pattern around the pinion and gear, indicating that there was runout in the pinion, gear, or both. The misalignment could be caused by lead error in the pinion, gear, or both, or by inaccuracy in the gear housing bores. Therefore, the HSP, HSG, and gear housing bores should be inspected to determine the source of the misalignment of the HS gear mesh. Endplay in the HS bearings A1/A2 was within specified tolerance. Therefore, bearing internal clearance did not contribute significantly to the misalignment.

Scuffing is rare in wind turbine gears. It is likely that it occurred in this gearbox when it lost oil and the HS gearset was momentarily starved of lubricant.

Sun spline fretting corrosion

Figures 7-8 show severe fretting corrosion on the sun spline. The damage was centralized on the spline teeth, but varied in severity around the spline, with only about 50% of the teeth carrying the load. The load zones were about 180° apart, indicating that the external or internal spline was out of round. The accuracy of the internal spline is expected to be lower than the external spline because it was shaper cut. Cutting is less accurate than grinding, and the internal spline was nitrided, which imparts some distortion.

Adhesion between the external sun spline and the hollow shaft internal spline transferred lumps of material from the hollow shaft. Axial sliding broke the welds and deformed the material in the axial direction. The red debris in Figure 8 is hematite (Fe_2O_3). Hematite is a polishing agent and it created the polishing wear that surrounds the fretting damage.

Because the external spline was carburized and ground, the internal spline was nitrided, and the spline was force-lubricated. It should have been resistant to fretting corrosion. Therefore, the root causes of the failure were probably lubricant starvation and poor load distribution.

Hollow shaft seal scuffing

Figures 9-11 show severe scuffing on the hollow shaft and the “O”-ring seal plate. Excessive endplay in the TRB bearings E1/E2 caused the hollow shaft to rub on the “O”-ring plate resulting in severe scuffing on the hollow shaft and “O”-ring seal plate. The “O”-ring vaporized.

Figures 12-13 show wear on the face of the bearing locknut. Abrasion removed 0.27 mm from the face of the locknut. The end face of bearing E1 IR also was worn, but to a much lesser degree than the locknut. Assuming the bearing endplay had been set to the specified endplay of 0.13 mm, the wear on the bearing locknut would have increased the endplay to 0.40 mm, which is consistent with the endplay of 0.41 mm measured during disassembly. Therefore, the root cause of the failure was excessive endplay in the TRB bearings E1/E2, which was caused by wear on the bearing locknut due to the spinning of the IR in bearing E1.

ANSI/AGMA/AWEA 6006-A03 [2] requires that all bearing fits be tight to prevent the spinning of the bearing rings. Therefore, the current design does not conform to ANSI/AGMA/AWEA 6006-A03 requirements. The design should be revised to use an interference fit on the IR of bearing E1 to prevent the spinning of the IR. Furthermore, the design of the locknut should be revised such that it applies a high axial clamping force.

Bearing A1 overheating

Figures 14-15 show that the IR raceway and the rollers of bearing A1 had straw-yellow temper colors. This indicates that the temperature reached about 400°F. The root cause of the overheating was probably lubricant starvation.

Bearing D assembly damage

Figures 16-17 show assembly damage on the IR of bearing D. ANSI/AGMA/AWEA 6006-A03 [2], Figure 5, shows the root cause of the damage, which is due to forcing the assembly of the bearing when the rollers are cocked. It is a risk associated with blind assembly. Assembly damage often leads to macropitting and failure of the bearing. Therefore, the assembly procedure for bearing D should be revised as necessary to avoid assembly damage.

Bearing D corrosion

Figure 18 shows contact corrosion at the roller spacing on the IR in bearing D. It occurs when free water is retained under a meniscus of oil in the converging gaps where the roller contacts the raceway. The corrosion proved that there was water in the lubricant. Therefore, the design of the lubrication system should be reviewed and revised as necessary to prevent ingress of moisture. For example, there should be V-ring seals on bearing caps A, E, and H, a felt seal in bearing cap A, and a desiccant breather on the gearbox.

Spacer assembly damage

Figures 19-20 show assembly damage on the OR spacer for bearings C1/C2. Therefore, the design of the spacer should be revised to avoid assembly damage.

Sun spherical thrust ring fretting corrosion

Figures 21-24 show fretting corrosion on the sun spherical thrust rings. Because the lower thrust ring was nitrided, and the thrust rings were force lubricated, they should have been resistant to fretting corrosion. Therefore, the root cause of the fretting corrosion was probably lubricant starvation due to malfunction of the bronze transfer ring. The design of the lubrication system should be revised as necessary to ensure an adequate oil flow rate to the sun spherical thrust rings. For example, the oil transfer ring for the hollow shaft should be revised to eliminate jamming.

Bearing H fretting corrosion

Figures 25-27 show fretting corrosion on the interface between bearing H OR and the shoulder on bearing cap H. The fretting corrosion extended over a 180° sector of the shoulder. Moderate fretting corrosion also occurred on a 140° sector of the outside diameter of bearing H OR. The root cause of the fretting corrosion was probably the loose fit of bearing H OR. Therefore, the design of the fit of the OR in bearing H and the bearing cap for bearing H should be revised as necessary to eliminate fretting corrosion.

Gear teeth fretting corrosion

Figures 28-29 show severe fretting corrosion on the sun pinion. Many gear teeth had similar damage. The root cause of the fretting corrosion was parking the wind turbine. Therefore, the wind turbine parking procedure should be revised as necessary to prevent fretting corrosion.

Gear teeth debris trapping

Figures 30-31 show fretting corrosion, polishing, and scuffing damage on the teeth of the INTP. The root cause of the damage was probably trapping of debris between a pair of teeth. The damage was imprinted on every tooth in the INT gearset because the gearset had a hunting gear ratio. Contamination by wear debris or gasket material should be eliminated to avoid damage to gear teeth and bearings.

Annulus gear scuffing

Figures 32-34 show scuffing damage on the teeth of the ANN. The root cause of the damage was probably trapping of debris between a pair of teeth. The damage was imprinted on every third tooth of the ANN gear because the gearset had a non-hunting gear ratio with a common factor of three. Contamination by wear debris or gasket material should be eliminated to avoid damage to gear teeth and bearings.

Annulus gear load flanks and wear pattern

Figure 35 shows some of the original macropits that were hand dressed. It is not clear why the damaged load flanks were used for the test gearbox. Since the ANN gear is symmetrical, it could have been reversed to use the original no-load flanks.

Figure 32 shows the ANN gear had grind marks and mild polishing wear at the generator end of the teeth, whereas Figure 35 shows the ANN gear had severe polishing wear that removed all traces of the grind marks and caused a wear step at the rotor end of the teeth. This indicates that there was misalignment between the ANN gear and the planet gears. Therefore, the lead modifications for the planet and ANN gear should be revised as necessary to improve load distribution on the planet/ANN gear mesh.

The damage is extensive on the ANN gear, and it should be replaced with a new gear.

Oil transfer ring jamming

Figures 36-38 show the oil transfer ring for the planet carrier. It was found cocked and jammed in the carrier. The wear pattern on its rubbing face showed it had only limited contact over a 50 mm sector with the housing. Hand pressure on the transfer ring showed that it was prone to jamming.

The oil transfer ring for the hollow shaft did not appear to be jammed. The wear pattern on its rubbing face showed it had nearly 360° contact with the housing. However, hand pressure on the transfer ring showed that it was prone to jamming.

The design of the oil transfer rings should be revised as necessary to eliminate jamming. Furthermore, a test should be designed to measure the oil flow rate to the planet bearings and sun spline.

ANN gear bolt torque

It was not possible to obtain accurate torques for the ANN bolts because they had been assembled with Loctite. Furthermore, upon disassembly, one ANN bolt on the HS housing interface jammed and stripped threads in the annulus gear (see Figure 39). Therefore, Loctite should not be used on the ANN gear bolts, and the access for the stripped ANN bolt should be reviewed and tools should be designed for assembly/disassembly of the bolt to prevent stripping of bolt threads.

ANN gear flat washers

The flat washers for the ANN bolts had their outside diameters reduced by machining (see Figure 40). This defeated the purpose of the washers and increased contact pressure on the cast iron housings. Therefore, large diameter hardened steel washers should be used on the ANN bolts. Furthermore, spot faces on the torque arm and HS housing should be machined to provide smooth, flat surfaces for the washers.

HS and LS shaft seals

Figures 41-43 show that there was no external V-ring and no felt seal on the HS labyrinth, and no external V-ring on the LS labyrinth. This allowed the gearbox to breathe through the labyrinths and ingest moisture and dust. Therefore, an external V-ring and felt seal should be added to the HS labyrinth and an external V-ring should be added to the LS labyrinth.

Carrier rust

Rust was found on the carrier bore for the rotor shaft and on the OD fit for the shrink ring (see Figure 43). This occurred because no rust preventative was applied when the gearbox was removed from the rotor shaft. Therefore, the bore and outside diameter of the carrier extension should be coated with rust preventative whenever the gearbox is disassembled from the rotor shaft.

Pitch tube bearing shields

Figure 11 shows that there was no shield on the inboard side of the pitch tube bearing. This allowed grease to leak out of the bearing into the gearbox. Therefore, the pitch tube bearing should be changed to one with double shields.

Provisions for assembly and disassembly

Provisions for assembly and disassembly were inadequate. Therefore, the gearbox design should be revised to provide features and tooling to assist assembly and disassembly such as, but not limited to:

- Add provisions for handling the hollow shaft
- Revise the hollow shaft such that bearing E2 IR is removable
- Revise the sleeve and spacer for bearings E1 and E2 to allow removal of the ORs
- Add provisions for measuring endplay on the INT and hollow shafts
- Use a rubber gasket on both inspection covers so that the housing surfaces are clean and no sealer is necessary
- Use silicone sealer or a ductile gasket material on bearing caps.

Dykem

Dykem spray was used. The coating thickness was too thick for accurate contact pattern inspection. Furthermore, there was excessive overspray on the gear housing and other components, which lead to misleading photos from the field tests. The photos seemed to show dark areas on the interior of the gear housing that were misinterpreted as burned interior paint caused by bearing overheating. However, Dykem remover readily removed the dark areas, proving that they were Dykem overspray.

Application of Dykem requires considerable skill to do it properly. Therefore, Dykem spray should not be used, and GEARTECH QP8702 [3] should be followed for applying Dykem.

Experiment to measure planet carrier displacement

Figure 44 shows the experimental setup used to measure the displacement of the planet carrier relative to the gear housing. The intent was to determine the angular displacement of the axis of the planet carrier relative to the axis of the ANN gear.

Two dial indicators, mounted 140 mm apart in the axial direction, probed the outside diameter of the carrier extension. The gearbox was fastened to the foundation of the test stand and the planet carrier was lifted with a strap attached to the overhead hoist.

The measurements were as follows:

Outboard indicator reading = 0.5334 mm

Inboard indicator reading = 0.4318 mm

Difference in indicator readings = 0.1016 mm

Angular displacement = $0.1016/140 = \underline{0.00073 \text{ radians}}$

Conclusions

A Jahnel-Kestermann gearbox was disassembled and inspected at The Gear Works in Seattle, Washington. The gearbox had been in operation in a turbine at the Ponnequin wind farm for several months. This report summarizes the results of the inspection, which have been entered into the GRC Failure Database. The report also presents recommendations for improvement in its design, which can be taken into consideration by the GRC in current gearbox redesign work.

References

1. H. Link, W. LaCava, J. van Dam, B. McNiff, S. Sheng, R. Wallen, M. McDade, S. Lambert, S. Butterfield, and F. Oyague, "Gearbox Reliability Collaborative Project Report: Findings from Phase 1 and Phase 2 Testing," NREL/TP-5000-51885, June 2011.
2. ANSI/AGMA/AWEA 6006-A03, "Standard for Design and Specification of Gearboxes for Wind Turbines," AGMA, 2003, pp. 1-94.
3. GEARTECH QP8702, "Inspection of Gear Tooth Contact Patterns with Hard Lacquer," Rev. B, 8/16/10, pp. 1-4.